OPEN

Recapitulating physiological and pathological shear stress and oxygen to model vasculature in health and disease

Hasan Erbil Abaci, Yu-I Shen, Scott Tan & Sharon Gerecht

Department of Chemical and Biomolecular Engineering, Johns Hopkins Physical Science Oncology Center and Institute for NanoBioTechnology, The Johns Hopkins University, 3400 N. Charles St., Baltimore, Maryland 21218, USA.

Studying human vascular disease in conventional cell cultures and in animal models does not effectively mimic the complex vascular microenvironment and may not accurately predict vascular responses in humans. We utilized a microfluidic device to recapitulate both shear stress and O_2 levels in health and disease, establishing a microfluidic vascular model (μVM). Maintaining human endothelial cells (ECs) in healthy-mimicking conditions resulted in conversion to a physiological phenotype namely cell elongation, reduced proliferation, lowered angiogenic gene expression and formation of actin cortical rim and continuous barrier. We next examined the responses of the healthy μVM to a vasotoxic cancer drug, 5-Fluorouracil (5-FU), in comparison with an *in vivo* mouse model. We found that 5-FU does not induce apoptosis rather vascular hyperpermeability, which can be alleviated by Resveratrol treatment. This effect was confirmed by *in vivo* findings identifying a vasoprotecting strategy by the adjunct therapy of 5-FU with Resveratrol. The μVM of ischemic disease demonstrated the transition of ECs from a quiescent to an activated state, with higher proliferation rate, upregulation of angiogenic genes, and impaired barrier integrity. The μVM offers opportunities to study and predict human ECs with physiologically relevant phenotypes in healthy, pathological and drug-treated environments.

H uman vascular disease is commonly studied using preclinical animal models, which do not fully represent human endothelial characteristics, or through conventional *in vitro* cultures of human endothelial cells (ECs), which are typically maintained at static and atmospheric oxygen (O_2) conditions. The EC microenvironment, however, is orchestrated by complex chemical and mechanical signaling making the achievement of physiological endothelial phenotype in conventional laboratory settings a difficult task. Shear stress, caused by blood flow, is one of the main regulators of EC phenotype and barrier integrity. Variations of shear stress levels in different regions of the arteries were shown to play a pivotal role in the formation of distinct phenotypes[1]. Long-term exposure of cultured ECs to physiological levels of laminar shear stress leads to various cellular responses such as cellular alignment with the direction of flow[2], improvement of endothelial barrier integrity[3], decreased proliferation[4] and upregulation of transcription factors such as Kruppel-like factor-2 (*KLF2*)[5], all of which are associated with EC phenotype *in vivo*[2,6]. On the other hand, ECs are also exposed to sub-atmospheric dissolved O_2 (DO) levels ranging from 5-12% O_2[7]. It is well established that the hypoxic conditions ($\leq$5%) alter endothelial phenotype and permeability[8–10]. We and others have shown that cultured ECs respond differently when at physiological O_2 (5–12%) compared to conventional atmospheric O_2 (21% O_2)[11–12]. Overall, while the individual effects of varying shear stress and O_2 tension on angiogenesis have been studied, creating an *in vitro* system with control over both shear stress and O_2 levels will advance our understanding and predictability of human endothelial functionality in healthy and diseased conditions.

Microfluidic technology offers an approach to precisely control the level, duration, and extent of various cues in the cellular microenvironment. In the last decade, EC maintenance in microfluidic systems has been established by a number of studies, as reviewed elsewhere[13]. These systems were designed to mimic different physiological factors such as hemodynamic forces, O_2 or co-culture in order to achieve an *in vitro* vascular model. However, none of these systems have focused on simultaneous control of shear stress and O_2 tension. Furthermore, only a small number of studies thoroughly demonstrated the establishment of an *in vivo* mimicking EC phenotype in physiological/pathological states[14–15]. In the first part of the study, we establish a microfluidic vascular model (μVM) recapitulating both physiological shear stress and O_2 levels in a device that was recently developed in our lab[16]. We begin by demonstrating time-dependent transition of human ECs from *in vitro* phenotype to

1

physiologically relevant phenotypes. To confirm the phenotypic similarity of the µVM to *in vivo*, we study endothelial responses to a vasotoxic chemotherapeutic drug, 5-Fluorouracil (5-FU; (20)) and to a vasoprotective agent Resveratrol[17] in the µVM and *in vivo*. In the past decade, long-term cardiotoxic adverse effects of chemotherapeutics including 5-FU have become a pivotal issue with the increased life span of cancer patients owing to progress in cancer treatment[18]. However, the mechanisms underlying direct effects of 5-FU on ECs is yet to be understood due to difficulties in clinical examinations and lack of physiologically relevant *in vitro* models.

Finally, we explore whether the µVM can also be used to create a vascular disease model. We propose that the µVM can accurately simulate atherosclerosis-associated ischemic conditions *in vitro* by simultaneously controlling shear stress and O_2 levels. In ischemic tissues, shear stress and O_2 tension reach low levels due to reduced or complete cessation of blood flow[19]. Stimulation of angiogenesis using proangiogenic recombinant proteins or adenoviral vectors containing proangiogenic transgenes has been used as a therapeutic approach to ischemic injury[20–21]. Although proangiogenic therapy has led to promising results in both preclinical and clinical trials, angiogenic responses to pathological microenvironments should be better understood in order to improve the therapeutic efficacy and to prevent commonly encountered complications such as vascular permeability and hypotension[21]. Therefore, *in vitro* models that allow for accurate simulation of ischemia by recapitulating the disturbed chemical and mechanical factors in vascular microenvironment are necessary.

Results

Establishing a microfluidic vascular model (µVM): phenotypic adaptation from conventional culture to physiological conditions. Using the capabilities of the microfluidic system previously developed in our laboratory[16], we mimicked healthy conditions where cultured cells can be maintained at physiological shear stress and O_2 tension (i.e. 12 dyn/cm² and 5% O_2 (38 mmHg)) as well as ischemic conditions (i.e. 0.01 dyn/cm² and 1% O_2 (7.6 mmHg)[22]) compared to conventional culture conditions (i.e. 0.01 dyn/cm² and 21% O_2 (159.6 mmHg)) as described in Figure 1A. The time points were initially chosen based on previous studies focused on the formation of continuous adherent junctions[23–24]. In addition, DO levels in the cell culture media were continuously monitored using O_2 sensor patches at the inlet and outlet of the microchannel[11,16,25] throughout the experiments at each condition (Figure 1B).

Using an improved microfluidic setup (Supplementary Figure 1), ECs were seeded and subjected to physiological shear stress and O_2 for two days. Time dependent changes in morphology, F-actin

organization, endothelial barrier integrity and localization of adherens junction proteins were examined to understand the phenotypic adaptation from conventional culture (i.e. 0.01 dyn/cm² and 21% O_2) to physiological conditions. After 24 hours at physiological conditions, ECs were elongated and aligned with the direction of the flow, continuing their elongation after 48 hours (Figure 2A). F-actin staining of the ECs demonstrated that most of the actin fibers were localized at the cell borders in conventional culture conditions (Figure 2B (ai)). After 24 hours in physiological conditions, we observed the formation of abundant and thicker actin stress fibers that were organized throughout the cytoplasm and aligned with the direction of the flow (Figure 2B (bi)). As the duration of the physiological conditions was extended to 48 hours, the stress fibers disassembled into shorter actin filaments and reorganized peripherally to form the cortical actin rim, indicating a more stabilized state of cell-cell contact (Figure 2B (ci);[26]). The morphology and organization of actin filaments were found to be comparable to that of an intact EC inner lining layer of mouse aorta (Figure 2B (di)). Intercellular gaps and localization of the vascular endothelial cadherin (VECAD) and platelet endothelial cell adhesion molecule 1 (PECAM1), which are adherens junctional proteins and responsible for mechanotranduction in ECs[2], were determined by immunofluorescent imaging. In conventional culture conditions, we observed an endothelial barrier integrity associated with VECAD localization at the cell borders. After 24 hours at physiological conditions, VECAD localization at the cell borders was compromised: the cell-cell contact occurred through membrane protrusions leading to a higher number of intercellular gaps (Figure 2B (a and b-e))[23–24]. In some regions of the membrane, we observed VECAD-positive linear structures extending into the cell (Figure 2B (bii)). These structures were orthogonal to the cell borders and co-localized with the ends of stress fibers, suggesting that stress fibers dynamically retract and release the adherens junction proteins, thereby mediating discontinuous adherens junctions[23,27]. After 48 hours at physiological conditions, VECAD protein was localized to the cell borders, reestablishing the continuous cell-cell contact (Figure 2B (c–e)). Both the number and size of intercellular gaps were decreased indicating an improved endothelial barrier integrity after 48 hours in physiological conditions (Figure 2B (fi–fii)). The localization and integrity of VECAD after 48 hours in physiological conditions resembled that of an intact EC inner lining layer of mouse aorta (Figure 2B (dii)) Although peripheral localization of PECAM1 did not increase after 48 hours, PECAM1 localized as thick structures at some regions of cell-cell contact (Supplementary Figure 2). This reticular organization of PECAM1 has recently been shown to contribute to endothelial barrier function[28]. Our gene expression analyses of the ECs exposed to
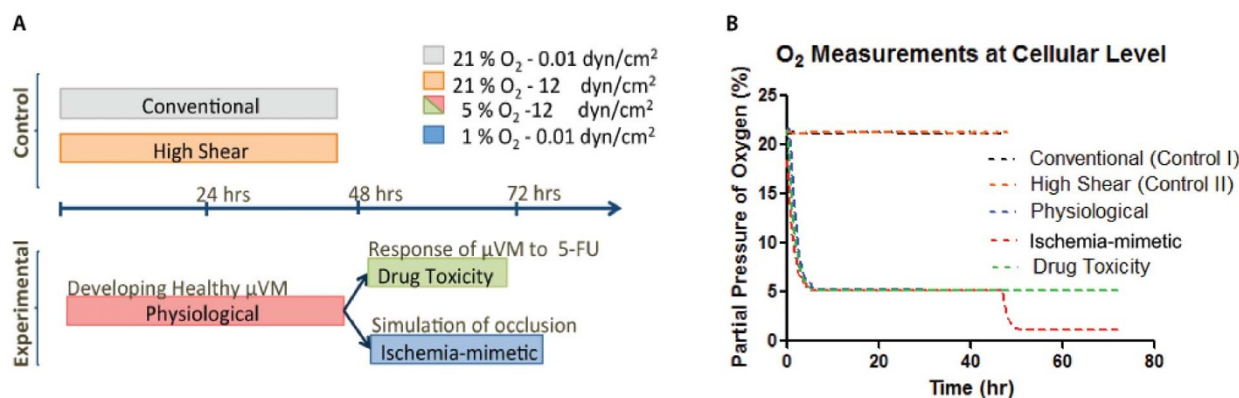

Figure 1 | Description of experimental conditions. (A) The timeline of shear stress and DO levels for each experimental condition is depicted: two control conditions (conventional and high shear), one healthy model (physiological) and two models for anti-cancer drug toxicity and ischemic vasculature. (B) DO level measurements in the culture media in the microfluidic system throughout each experimental condition demonstrating control over targeted DO levels.
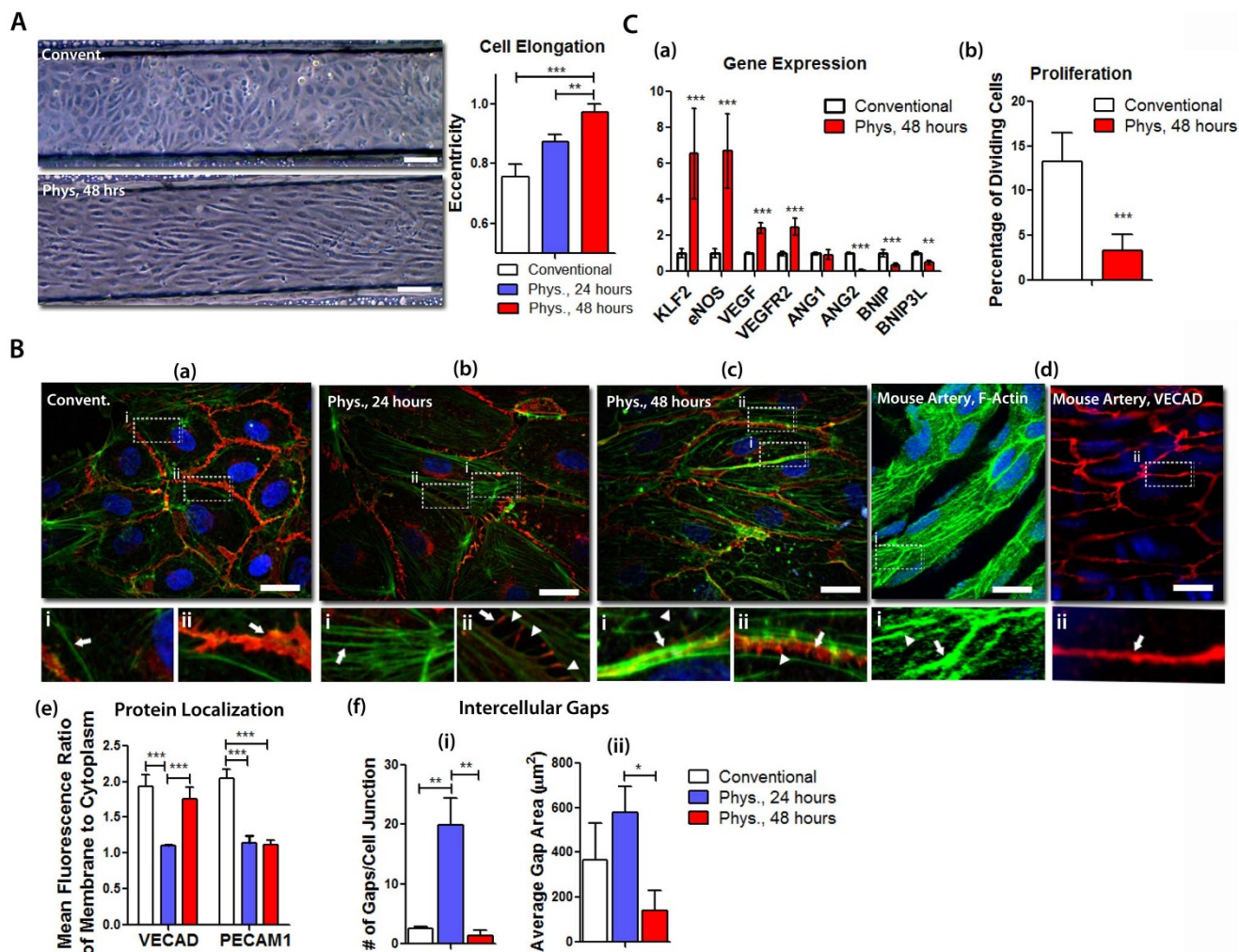
Figure 2 | Development of the *in vitro* μVM model at physiological shear stress and oxygen tension. (A) Light microscopy images of ECs cultured in conventional conditions or physiological conditions in the μVM for 48 hours and cell elongation index (eccentricity). Scale Bar: 100 μm (B) High resolution immunofluorecent imaging of VECAD (red), F-actin (green) and DAPI (blue) in ECs cultured at (a) conventional conditions, (b) physiological conditions for one day (Phys, 24 hrs) and 48 hours (Phys, 48 hrs), compared to (d) inner EC lining of mouse artery revealed the EC adaptation to physiological conditions in terms of F-actin organization: ai - cortical actin, bi - stress fibers, ci and di - cortical actin rim (indicated by arrows in the respected images) and short actin filaments (arrowheads) and in terms of adherens junctions: aii - continuous adherens junctions, bii - membrane protrusion, cii and dii - reestablished adherens junctions (indicated by arrows in the respected images) and intercellular gaps (arrowheads); (e) the peripheral localization of adherens junction proteins and (f) the number and area of intercellular gaps were quantified using the immunofluorescent images. Scale bar: 20 μm (C) Transition of ECs to *in vivo* mimicking phenotype after 48 hours at physiological conditions was examined by quantitative RT-PCR to determine mRNA levels of relevant genes and by Ki-67 staining to determine the percentage of dividing cells. All data was compared to ECs cultured at conventional conditions in the μVM (mean ± SD, *p < 0.05, **p < 0.01, ***p < 0.005).

physiological conditions for 48 hours showed that both *KLF2* and *eNOS* were significantly upregulated compared to conventional culture conditions, indicating a transition to *in vivo* phenotype (Figure 2C (a)). Similarly, *VEGF* and *VEGF* receptor-2 (*VEGFR2*) were slightly upregulated, in agreement with previous studies suggesting the anti-apoptotic role of increased autocrine levels of VEGF and VEGFR2[29]. Angiopoietin 1 (*ANG1*), which is responsible for vascular maturation and barrier function, was not affected by the physiological conditions whereas *ANG2*, an antagonist of *ANG1*, was dramatically downregulated compared to conventional culture conditions. This finding is consistent with the analyses of intercellular gaps suggesting that physiological conditions promote improved endothelial barrier integrity similar to that found in the body (from Figure 2B (dii)). Finally, we found that the percentage of dividing ECs was significantly lower after two days in physiological conditions suggesting a transition to quiescent state (Figure 2C (b)). Altogether, we establish an *in vitro* μVM and demonstrate its ability

to achieve *in vivo* EC phenotype within 48 hours at physiological shear stress and O₂ tension.

Responses of μVM to vaso-effective drugs: Administration of 5-FU impairs endothelial barrier integrity that can be alleviated by co-administration of Resveratrol. 5-Fluorouracil (5-FU) is a broadly administered anti-cancer drug targeting a wide range of solid-organ tumors including those found in gastrointestinal and breast cancer[30]. Although cardiotoxicity of 5-FU is well-documented as 10% of the patients treated with this drug suffered from myocardial infarction, ischemia, congestive heart failure or sudden cardiac death, the mechanisms underlying the toxicity is not understood[18]. Noncardiac vascular toxicity caused by the drug has been investigated by a limited number of studies using either animal models[31] or *in vitro* using conventional cultures of ECs[31]. We sought to examine the response of the healthy μVM to 5-FU toxicity by examining the underlying mechanisms in comparison with an *in vivo* mouse
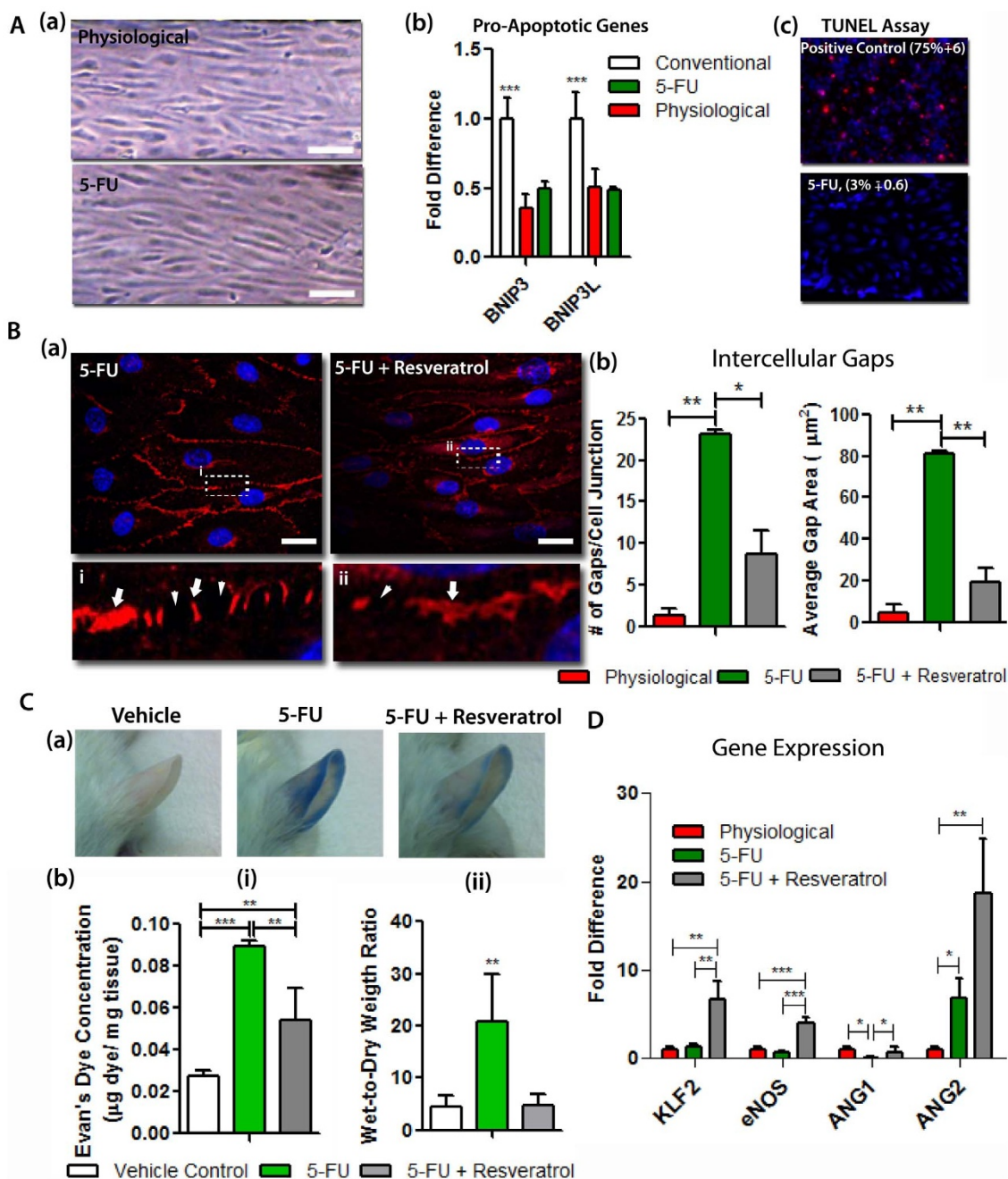
Figure 3 | Administration of 5-FU impairs endothelial barrier integrity that is alleviated by co-administration of Resveratrol. (A) The apoptotic effect of 5-FU was examined on ECs cultured in physiological condition for 48 hours. (a) Inverted microscope images of ECs cultured in the μVM with and without 5-FU. Scale bar: 100 μm. (b) quantitative RT-PCR was performed to compare pro-apoptotic gene expression in ECs cultured in conventional conditions, physiological conditions or with 5-FU. (c) TUNEL assay was performed to detect apoptotic cells. The percentage of apoptotic cells after 5-FU treatment was compared to ECs treated with DNAse as the positive control. (B) (a) Fluorescent images of VECAD (red) and nucleus (blue) of ECs cultured in μVM demonstrate that (i) adherens junctions (arrows) were disrupted by treatment with 5-FU leading to the formation of intercellular gaps (arrowheads) and (ii) co-administration of 5-FU and Resveratrol alleviated the formation of discontinuous adherens junctions (arrows) and intercellular gaps (arrowheads). (b) the number and area of intercellular gaps were quantified using the immunofluorescent images. (C) *In vivo* experiments in mouse confirm the hyperpermeability effect of 5-FU alone and vasoprotective role of adjunct Resveratrol therapy. (a) Evans blue dye leakage in the ears of mice 20 minutes after the application of mustard oil. (b) Extravasated concentration of (i) Evans blue dye and (ii) water accumulation in the lungs of mice. (n = 5) (D) RT-PCR analyses of human ECs cultured in the μVM allowed for examining mRNA levels of the genes that are potentially responsible for the observed effects of drug treatment.

model. After 48 hours in physiological conditions, 5-FU was added to the media in the μVM for 24 hours at a clinically relevant concentration of 7 mM[32–33]. We could not detect cell detachment or changes in cell morphology in response to 5-FU (Figure 3A (a)). The expression levels of pro-apoptotic genes, BCL-2/

adenovirus E1B 19-kDa-interacting protein 3 (*BNIP3*) and BNIP3-like protein (*BNIP3L*), were downregulated compared to conventional conditions and were similar in both physiological conditions and 5-FU treated cells (Figure 3A (b)). TUNEL assay also showed that the ECs cultured in physiological conditions did not undergo

apoptosis in response to treatment with 5-FU (Figure 3A (c)). As this data demonstrated that 5-FU does not induce EC apoptosis, we continued to explore potential effects of 5-FU on EC phenotype. Performing high-resolution imaging analyses of the adherens junctions, we found that 5-FU increases both the number and area of intercellular gaps compared to physiological conditions, suggesting that 5-FU may lead to hyperpermeability of blood vessels (Figure 3B (a–b)). Resveratrol is a natural chemical that has recently been shown to enhance the efficacy of 5-FU on inhibition of tumor growth[34]. There is also a growing body of evidence that Resveratrol has protective effects against disruption of endothelial barrier function[17,35–36]. Thus, we hypothesized that co-administration of Resveratrol may overturn intercellular gap formation caused by 5-FU. We administered Resveratrol at a concentration of 100 μM in combination with 5-FU. After 24 hours of combination treatment, both the number and area of intercellular gaps were decreased, compared to treatment with 5-FU alone, suggesting a vasoprotective role of Resveratrol in 5-FU treatment (Figure 3B(aii) and (b)). In control experiments in which 5-FU treatment was applied to conventional petri-dish cultures, we observed a similar hyperpermeabiltiy effect of 5-FU (Supplementary Figure 3). However, using Resveratrol in combination with 5-FU did not overturn the formation of intercellular gaps induced by 5-FU, as opposed to Resveratrol's suggestive protective role demonstrated in the μVM. In order to determine whether Resveratrol is vasoprotective, we performed the experiments *in vivo* by examining the vascular permeability of microvasculature and descending aorta in treated mice. Mice were injected with 5-FU alone (60 mg/kg) or co-administrated with Resveratrol (6.5 mg/kg) for 24 hours. Intravenous tail vein injection of Evans Blue dye revealed vascular leakage in the ears of the mice treated with 5-FU alone whereas the co-administration with Resveratrol alleviated the level of the vascular leakage (Figure 3C(a)). In addition, extravascular concentration of Evans Blue dye in the lungs was significantly higher in the mice treated with 5-FU alone compared to vehicle control (Figure 3C (bi)). Similarly, wet-to-dry weight ratio of the lungs was also increased by 5-FU treatment indicating elevated water accumulation in the lung tissue as a response to 5-FU (Figure 3C (bii)). Moreover, examining the Concanavalin A (Con A) binding throughout the layers of the descending aorta revealed that 5-FU also causes a slight increase in the permeability of the EC monolayer (Supplementary Figure 4 (a)). These data agreed with our findings using the *in vitro* μVM. Overall, these results suggest that the μVM better mimics the response of healthy ECs to drug treatment than conventional experiments, and therefore allows obtaining predictive cellular responses. We next sought to use the *in vitro* μVM to begin exploring the underlying mechanism leading to the hyperpermeability response of human ECs to 5-FU. Previous reports suggested that 5-FU causes vasoconstriction which can be prevented by stimulation of eNOS content and activity[31]. Therefore, we first examined the mRNA levels of *KLF2* that mediates *eNOS* expression[31,33]. Interestingly, the expression levels of *KLF2*, which is also a key factor found in healthy ECs *in vivo*[5], and *eNOS* in human ECs were not affected by the administration of 5-FU (Figure 3D). We also validated the unchanged expression levels of *eNOS* in response to 5-FU in ECs of mouse aorta (Supplementary Figure 4 (b)). The gene expression levels of *VEGF* and *VEGFR2* were also not affected in human ECs by 5-FU or adjunct Resveratrol therapy (Supplementary Figure 5). On the other hand, 3-fold increase in *ANG2* expression levels accompanied with the significant downregulation of *ANG1* expression in response to 5-FU. Recent hypothesis suggests that ANG1/ANG2 ratio is a more critical parameter than absolute levels of individual proteins for controlling vascular permeability[37]. Thus, our data highlighted the possibility that dramatically decreased *ANG1/ANG2* ratio of 0.022 ± 0.003 after 5-FU treatment compared to 15.2 ± 1.3 in physiological

conditions may be the mechanism responsible of discontinuous adherens junctions in response to 5-FU (Figure 3D). After the combination treatment with Resveratrol, *ANG1/ANG2* ratio increased to 0.041 ± 0.01, which was significantly higher than that in 5-FU treatment, whereas it still remained lower than the levels in physiological control. Although we suggest that decreased *ANG1/ ANG2* ratio can be a potential mediator of the hyperpermeability effect of 5-FU, the mechanism behind the recovering effect of Resveratrol still remains unknown. One potential mediator of this may be myosin light chain phosphorylation which was shown to be both responsible for hypermeability of ECs[38] and inhibited by Resveratrol by several studies[39–40]. Interestingly, Lin et al[41] also showed that overexpression of KLF-2 inhibits EC hyperpermeability through MLC phosphorylation. The profound upregulation of KLF-2 after Resveratrol treatment (see Figure 3D) also agrees with this hypothesis. Additional studies, however, are required to elucidate the precise mechanism underlying the effects of these drugs on vascular permeability.

Simulation of atherosclerosis-driven ischemia leads to human EC activation. Atherosclerosis-associated occlusion of arteries leads to myocardial or cerebral ischemia, which may cause lethal damage to heart and brain tissues. Angiogenesis, the formation of blood vessels from pre-existing ones, occurs in ischemic tissues where the surrounding blood vessels experience a simultaneous decrease in shear stress and dissolved O_2 levels[42]. Here, we utilized the μVM to determine the dynamics of morphological and molecular changes in human ECs by recapitulating abnormal shear stress and O_2 levels found in ischemic tissues.

Following achievement of *in vivo* EC phenotype after 48 hours in physiological conditions, we simulated ischemia by simultaneously lowering the shear stress and O_2 levels to 0.01 dyn/cm^2 and 1% O_2, respectively. We found that after 24 hours in ischemia-mimetic conditions, VECAD distribution along the EC borders was significantly lower compared to its distribution along EC borders cultured in physiological conditions, whereas the localization of PECAM1 was not affected (Figure 4A (a)). Moreover, compared to physiological conditions (from Figure 2B (c)), we observed a decrease in the elongated morphology of ECs in response to ischemic conditions (eccentricity = 0.83 ± 0.023; Figure 4A (bi)). In fact, we observed two distinct cell populations in response to 24 hours of ischemia-mimetic conditions in terms of morphology, F-actin organization and cell-cell contact. In one population, the ECs were closely in contact with neighboring cells and occupied relatively small surface area similar to the morphology typically observed in confluent ECs in conventional cultures (from Figure 2B (a)). F-actin was randomly distributed in the cytoplasm as opposed to the peripheral F-actin distribution observed in conventional conditions (Figure 4A (bii)). In the second distinct population, the cells retained their elongated morphology; however, thick stress fibers were formed across the cytoplasm and oriented in the flow direction (Figure 4A (biii)). The cell-cell contact occurred through membrane extensions leading to a significant increase in the average number of intercellular gaps, compared to physiological conditions, indicative of a disrupted barrier integrity (Figure 4A (biii) and 4A (c)). Hypoxia (1%O_2) in conventional cultures in petri-dish did not induce intercellular gap formation, and resulted in a similar morphology and cell-cell contact to the first population we observed with μVM (Supplementary Figure 6), further suggesting that the μVM is superior to conventional cultures to more accurately mimic *in vivo* cellular responses.

We examined the expression levels of *KLF2*, *eNOS* and several angiogenic genes, which are controlled by shear stress and/or O_2 tension[5,43]. Kruppel like factor- 2 is a transcription factor, which is highly expressed in physiological phenotype of ECs and regulates the expression of a wide variety of genes including *eNOS* and angiogenic factors such as *VEGF* and *VEGFR2*[6,44]. Indeed, *KLF2* and *eNOS*
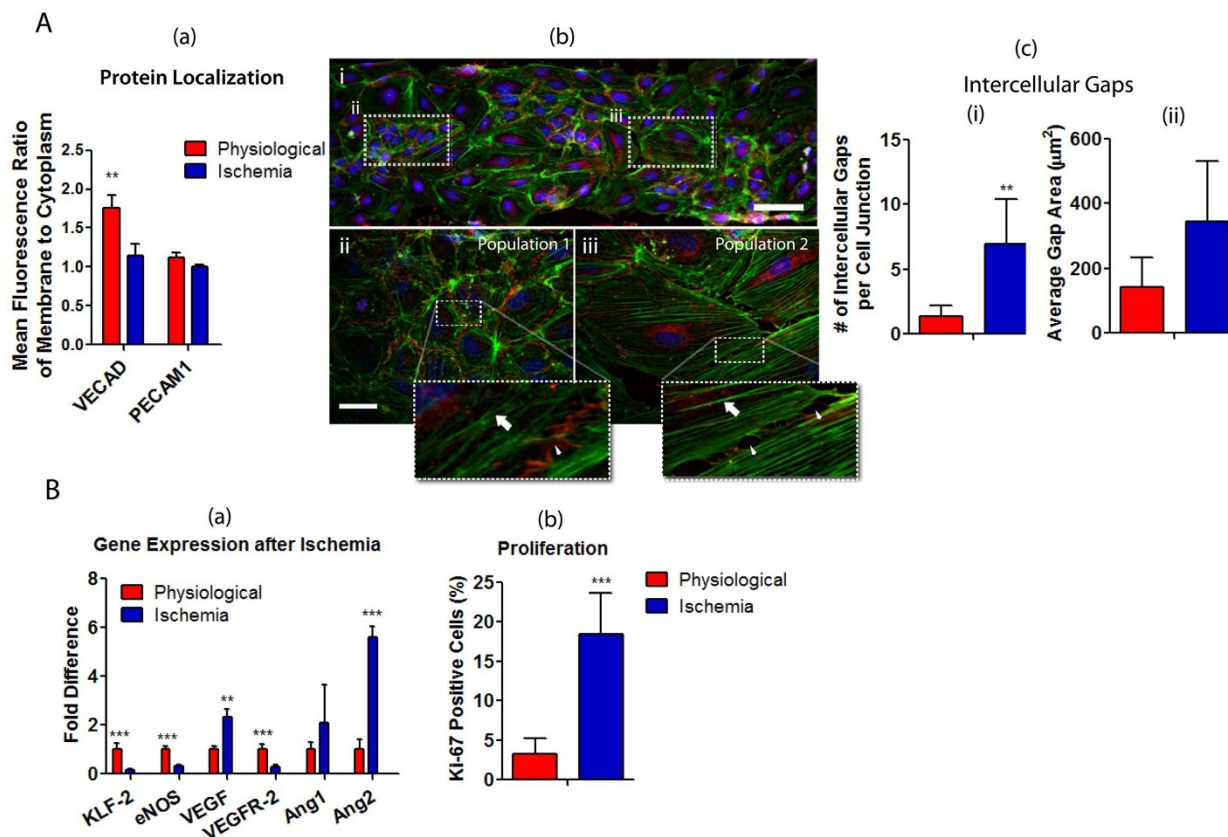
Figure 4 | Endothelial cell activation in response to simulated ischemia-mimetic conditions. (A) Ischemia was simulated using the *in vitro* μVM by lowering the shear stress and DO levels simultaneously to 0.01 dyn/cm^2 and 1% O_2, respectively, after achievement of *in vivo* mimicking phenotype in physiological conditions. High resolution fluorescent images of ECs after 24 hours in ischemia-mimetic conditions were analyzed for (a) the peripheral localization of adherens junction proteins and (bi) morphological changes compared to physiological conditions (Scale Bar: 100 μm), demonstrating the formation of two morphologically distinct cell populations (panels below are higher magnification images for the boxed area): bii - randomly distributed F-actin (arrow) and continuous adherens junctions (arrowhead) and biii - stress fibers (arrow), and intercellular gaps (arrowheads). Scale bar is 20 μm; (c) the number and area of intercellular gaps were quantified using the immunofluorescent images. (B) Angiogenic responses of ECs to 24 hours in ischemia-mimetic conditions was examined by quantitative RT-PCR to determine mRNA levels of angiogenic genes and by Ki-67 staining to determine the percentage of dividing cells. All data was compared to ECs cultured at physiological conditions in the μVM for 48 hours (mean ± SD, *p < 0.05, **p < 0.01, ***p < 0.005).

expression were significantly downregulated in ECs after 24 hours in ischemia-mimetic conditions, while the expression of *VEGF* and *ANG2* were found to be upregulated and the expression of *ANG1* remained unchanged. The role of *ANG2* in destabilization of quiescent ECs has been shown previously[45]. Thus, upregulation of *ANG2* in ischemia is consistent with the disrupted barrier integrity. Interestingly, *VEGFR2* expression levels were lowered by ischemia-mimetic conditions, compared to physiological conditions, reaching expression levels similar to the levels found in ECs cultured in conventional conditions (Figure 4B (a)). Twenty-four hours in ischemia-mimetic conditions also induced transition from quiescent to proliferative state of the ECs as indicated by increased percentage of Ki67-positive cells (Figure 4B (b)). Together these data demonstrate the growing ischemia-driven transition of ECs to an activated state where the endothelial barrier integrity is impaired, cell proliferation is increased, and angiogenic factors, such as *VEGF* and *ANG2*, are upregulated.

Discussion

We have established an *in vitro* μVM to study human vascular diseases such as atherosclerosis-driven ischemia as well as to accurately test the efficacy and toxicity of therapeutics. The μVM efficiently recapitulates physiological and pathological vascular microenvironments via simultaneous control of shear stress and O_2 levels.

Although other microfluidic systems have been successfully developed to mimic physiological shear stress on ECs[46–47], the μVM in this study is the first one, to our knowledge, that permits the simultaneous manipulation of shear stress and O_2 tension to produce physiological and pathophysiological EC phenotypes. In the body, ECs experience sub-atmospheric O_2 levels (<21%) ranging between 5–12%. Thus, in this study, we used a physiologically relevant O_2 tension of 5% and achieved a healthy human μVM with a quiescent, anti-apoptotic and athero-protective endothelial phenotype. However, we did not see significant differences between ECs cultured at physiological and high shear conditions in terms of morphology and mRNA levels (data not shown). Previous studies demonstrated the varying EC responses when cultured at physiological O_2 tensions[11–12]. A few previous studies also suggested synergistic effects of physiological shear stress and O_2 levels on ECs by pre-treating ECs with low O_2 prior to onset of shear stress[48] or using a parallel-plate flow system with preconditioned cell culture media at desired O_2 tension[49]. Although physiological O_2 tension did not influence the transition from the *in vitro* to *in vivo* phenotype in our study, it may be specifically critical especially when studying diseased conditions that involve O_2 fluctuations, and therefore influence the dynamics of O_2 species generation and nitric oxide release[50].

We validated the physiological proximity of the μVM to *in vivo*, also in terms of its responses to a broadly studied vasotoxic

chemotherapeutic drug, 5-FU, (20) and to a vasoprotective agent Resveratrol[17]. The anticancer drug, 5-FU, is a well-documented symptomatic cardiotoxin in patients. A very recent systematic review reported that symptoms of cardiotoxicity were detected in up to 20% of patients receiving 5-FU[51]. Yet, the mechanisms underlying the pathophysiology are not well understood. Although the majority of the clinical studies focuses on toxicity of 5-FU on cardiac tissue, some studies also highlighted that 5-FU may cause vascular injury by leading to a procoagulant state[52], vasocontractions[53], and even EC apoptosis[54] at relatively high doses. These studies provided clinical evidence to vasotoxicity of 5-FU and proposed vascular dysfunction as a possible mechanism behind the symptomatic cardiotoxicity. We first examined immediate pro-apoptotic role of 5-FU on ECs using the μVM. We observed no indication of apoptosis after 24 hours of treatment. While some studies detected apoptosis of cardiocytes[55] and central nervous system progenitors[32] at similar concentrations of 5-FU, Wada et al.[56] showed that 5-FU is anti-proliferative but not pro-apoptotic on HUVECs, in agreement with our data. Another study using a rat model of intra-arterial perfusion[54] showed EC apoptosis in response to intra-arterial perfusion of 5-FU. This response, however, was observed after 7 days and only near to the tip of the catheter where the ECs are exposed to much higher concentrations of 5-FU compared to complete dilution in blood.

Previous reports suggested that the vasoconstriction caused by 5-FU is endothelial-independent[33] and stimulation of eNOS by exercise training can potentially reverse this adverse effect[31]. Thus, we examined mRNA levels of *eNOS* and its transcription factor *KLF2* and did not detect a significant effect of 5-FU on these genes compared to physiological levels. We subsequently confirmed unaffected levels of *eNOS* in a mouse model suggesting that vasoconstriction is not through *eNOS* expression, supporting the previous evidence of endothelial-independent vasoconstriction. However, changes in the activity of eNOS and nitric oxide production and release should be further investigated.

The capability of performing high-resolution image analyses in the μVM system allow us to examine morphological and structural changes in response to 5-FU. We found that 5-FU induces intercellular gap formation indicating compromised endothelial barrier integrity. We also confirmed the toxic effect of 5-FU in a mouse model by showing extensive plasma leakage and accumulation in lungs. To our knowledge, this is the first study suggesting the hyperpermeability effect of 5-FU. Vascular hyperpermeability caused by 5-FU treatment may result in inflammation and contribute to complications of acute respiratory distress syndrome[57] and ischemia/reperfusion injury[58]. In addition, induction of leaky blood vessels in tumors can limit targeted delivery of the drug and lead to cancer metastasis[59]. As a possible solution, we showed that 5-FU- induced hyperpermeability can be alleviated by combined treatment with Resveratrol both in the μVM system and in a mouse model. Resveratrol was previously shown to reduce high-glucose[17], tumor necrosis factor-alpha[35] and staphylococcal enterotoxin B-induced[36] vascular hyperpermeability *in vitro* and *in vivo*, supporting the vasoprotective role of Resveratrol observed in this study. Interestingly, a recent report demonstrated that combined 5-FU treatment with Resveratrol decreases tumor size to a greater extent than 5-FU only[34]. While the authors attributed this effect to enhanced chemosensitivity of cancer cells by Resveratrol based on their *in vitro* experiments, it may be that the alleviation of vascular hyperpermeability by Resveratrol is a secondary possible mechanism underlying the enhanced response to the chemotherapy. We thus propose adjunct therapy for 5-FU by the co-administration of Resveratrol as a vasoprotecting strategy.

The capability of the μVM to manipulate shear stress and O$_2$ tension independently allowed us to mimic pathological conditions found in the ischemic tissue. Several *in vivo* studies demonstrated that two different types of neovascularization occur at the occlusion site and post-occlusive ischemic tissue[19,42]. It was suggested that new capillary formation is only observed in the ischemic tissue while collateral formation is found in the site of occlusion. These findings support the idea that the perturbation of shear stress and O$_2$ may be the driving force for the site-specific angiogenesis. Our simulations of ischemic conditions using the μVM revealed the morphological, structural and genetic changes leading to EC activation. Proliferation of ECs was detected previously in animal models to occur as early as 24 hr after exposure to low shear stress and O$_2$ levels, reaching a maximum number of proliferative ECs on day 3[60]. The proliferative response is usually associated with increased levels of growth factors, such as VEGF, released by the surrounding non-ECs including macrophages[61]. In our *in vitro* μVM, we show that ECs switch from quiescent to proliferative state merely as a result of changing physical conditions. These data suggest that initial proliferative response of ECs may be controlled by the lowered shear stress and O$_2$ tension in the ischemic tissue while it is accelerated at later stages as a response to released growth factors by surrounding cells.

Moreover, we observed two morphologically distinct populations of cells after 24 hours of ischemia. *In vivo* studies previously demonstrated the temporal and spatial profile of EC activation during ischemia[9,60-61]. In one study, ANG2 overexpression was only detected in individual ECs in the first 6–24 hrs of ischemia while prolonged ischemia of 3 days resulted in overexpression of ANG2 by all ECs[61]. We found a similar increase in mRNA levels of *ANG2* after 24 hrs of low shear stress and O$_2$ tension, which is in consistent with the intercellular gap formation we observed. In addition, after 24 hours, we determined a profound decrease in mRNA levels of *KLF2*, which was shown to inhibit VEGF-mediated[62] and hypoxia–induced[63] angiogenesis. Interestingly, *eNOS* and *VEGFR2* levels, in our study, were also found to be downregulated by low shear stress and O$_2$ tension. Previous studies, however, demonstrated the predominant positive role of *eNOS* and *VEGFR2* in angiogenesis during tissue repair and ischemia[64-65].Thus, our data can be interpreted as follows; *eNOS* levels are independently downregulated by lowered shear stress and O$_2$ tension, while exogenous growth factors, such as VEGF and TGF-β, are released in the tissue by surrounding cells in response to hypoxia to promote angiogenesis via upregulation of eNOS[66] and VEGFR2[65] in ECs. On the other hand, individual effects of lowered shear stress and O$_2$ tension on angiogenesis have extensively been studied. Some previous studies, for example, reported that lowered shear stress at atmospheric conditions (21% O$_2$), as occurs in lung-ischemia, causes angiogenic responses through reactive oxygen species generation and signaling[67]. Similarly, hypoxia has been shown to promote new vessel formation[68]. Although we primarily examined the synergetic effects of shear stress and O$_2$, individual contributions of these factors in the observed endothelial responses can further be investigated using the ischemic μVM. In addition, the ischemic μVM can potentially be used to determine correct dosage and combination of potential therapeutic agents, by testing the efficacy directly on human ECs under relevant physical conditions and by examining typically encountered complications, such as hyperpermeability.

Methods

See on-line supplementary for complete Materials and Methods.

Cell Maintenance in μVM. All components of the system were autoclaved separately and further sterilized with ethanol for 10 minutes after assembly. The glass surface of the device was coated with Fibronectin (10 μg/ml) prior to cell seeding. Cell seeding was achieved by injecting a cell suspension with a density of 5 million cells/ml. After 3 hrs of attachment period, growth media was supplied at a flow rate of 0.01 ml/hr overnight using a syringe pump (Chemyx, Stafford, TX). In static control experiments, the flow rate was maintained at 0.01 ml/hr, which is sufficient to provide nutrients and exerts a negligible shear stress of 0.007 dyn/cm^2 [25]. In high shear and physiological condition experiments, media was circulated at a flow rate of 20 ml/hr between the microbioreactor and a media reservoir using a peristaltic pump (Ismatec, Wertheim, Germany). Physiological O$_2$ was generated by continuously flushing both the microbioreactor and the media reservoir with a medical grade gas

mixture (5% CO_2, 1% O_2 and balance N_2). Ischemic conditions were created by lowering the shear stress and O_2 tension simultaneously to 0.01 dyn/cm^2 and 1% O_2 (5% CO_2, 5% O_2 and balance N_2). Drug treatment was performed by injecting 5-FU alone (Sigma-Aldrich, St. Louis, MO) or 5-FU and Resveratrol (Sigma-Aldrich) together directly into the media reservoir to give a clinically relevant concentration of 7 mM[32–33] and 100 μM[69], respectively.

Immunofluorescent Staining and Imaging. We analyzed the cellular morphology and protein localization using fluorescent imaging of fixed cells as previously[11,16,25]. All solutions used in fixation and staining steps in the μVM were injected at a flow rate of 1 ml/hr for a volume of 300 μl. Cells were first fixed with 3.7% paraformaldehyde solution for 2 hours at room temperature, permeabilized with 0.1% Triton X-100 for 15 minutes and then stained with Phalloidin (1 : 40) and 4 = 6-diamidino-2-phenylindole (DAPI) (1 : 1,000) to visualize the cytoskeleton and nuclei, respectively. For immunofluorescent labeling, cells were incubated for 2 hours with anti-human PECAM1 (1 : 100; Sigma-Aldrich) or VECAD (1 : 200; Santa Cruz Biotechnology, Santa Cruz, CA) and rinsed with phosphate buffer saline (PBS) followed by incubating with anti-mouse IgG Cy3 conjugate (1 : 50; Sigma Aldrich) for 1 hour. The fluorescently labeled cells were examined using fluorescence microscopy (Olympus BX60; Olympus, Center Valley, PA).

We performed fluorescent staining of *in vivo* tissue samples for analyses of cellular morphology. Mouse arteries were fixed immediately in ice cold 3.7% paraformaldehyde for 2 hours. Connective and adipose tissue around artery segments were removed and the artery was cut longitudinally using micro scissors under the dissecting microscope. Samples were then permeabilized with 0.1% Triton X-100 for 30 minutes. For immunofluorescent labeling, cells were incubated overnight with anti-mouse VECAD (1 : 200; Sigma-Aldrich), rinsed with PBS, and incubated with anti-goat IgG Cy3 conjugate (1 : 50; Sigma-Aldrich) for 2 hours. For *en face* imaging, samples were mounted on a glass slide using mounting medium (Dako, Glostrup, Denmark) ECs facing up. The fluorescently labeled arteries were examined using confocal microscopy (LSM 510 Meta; Carl Zeiss).

Quantification of Proliferation, Protein Localization, Cell Elongation and Intercellular Gaps. To identify the protein localization, the cellular membrane and nucleus were manually distinguished using the software CellProfiler (Broad Institute, Cambridge, MA). The cytoplasm was identified subtracting the region of the nucleus from the region surrounded by the cellular membrane. Protein localization was determined by calculating the ratio of the mean fluorescence intensities of the adherens junction proteins located at the cellular membrane edge and cytoplasm. The detailed image analyses using CellProfiler software used as previously described[70]. Changes in morphological elongation were assessed through comparing the eccentricity, measure of the deviation of a conic section from a circle, using Cell Profiler. Eccentricity is equal to zero for a circle and one for a parabola.

Intercellular gaps were identified using VECAD fluorescence at the magnification of 100X, as extracellular regions absent of VECAD fluorescence and surrounded on all sides by cellular membranes of two or more adjacent cells. Gap area and number were measured highlighting the individual gaps manually in ImageJ and normalized to the number of cells and averaged across all images. The number of proliferating cells was determined by counting the Ki-67 positive cells in the immunofluorescent images.

Mouse Drug Treatment. All experimental animal protocols were approved by the Institutional Animal Care and Use Committee at Johns Hopkins Medical School. 8–10 week old BALB/c mice (Charles River, Wilmington, MA) received three consecutive intravenous injections of 5-FU (60 mg/kg dissolved in 1% DMSO) or 5-FU and Resveratrol (6.5 mg/kg dissolved in 1% DMSO) every other day for mRNA extraction studies and single injection for the other analyses. Control animals were treated with equal amounts of PBS or 1% DMSO in PBS (vehicle control). The drug doses were determined to achieve the same clinically relevant drug concentrations used in the *in vitro* experiments. The average drug concentration in blood stream was calculated based on the first order clearance rates of 5-FU (16.4 μg ml^{-1} hour^{-1}) and Resveratrol (6.84 μg ml^{-1} hour^{-1}) from the blood[71–72]. Animals were then sacrificed the day after the final injection. Prior to harvesting the tissue of interest for analyses, *vena cava* was cut and intra-cardiac injection of ice-cold PBS was performed to remove the blood.

Vascular Permeability in Mice. Permeability of mouse microvasculature was analyzed by injecting Evans blue dye (30 mg/kg in 150 in PBS; Sigma Chemical Co.) intravenously into mice one day after injection of a single dose of 5-FU alone or 5-FU and Resveratrol. Ten minutes after the injection of the dye, mustard oil (Sigma Chemical Co.) diluted to 5% in mineral oil was applied to the surfaces of the ear. The pictures of the ears were taken after 20 minutes. Mice were sacrificed 30 minutes after the injection of the dye. The Evans blue dye was extracted from the intestines, lungs and liver by incubating the organs in 1 ml of Formamide (99.5%, Sigma Aldrich) overnight at 60°C and measured using spectrometer at 620 nm. The amount of extravasated dye per weight of tissue was calculated for comparison between samples. Water accumulation in different organs was examined by measuring wet-to-dry weight ratio. The wet weights of lung, intestines and liver were measured immediately after removal of the organs. The dry weight of the organs was measured after evaporation of the water in the organs at 60°C for 48 hours.

Concavalin A binding was used to assess the endothelial barrier function of descending aorta in a similar manner shown by others[73]. The aorta segments were first fixed in 3.7% paraformaldehyde, cut longitudinally, and mounted as flat on a glass slide with the lumen side of the vessels facing up. The sample was then blocked by 5% BSA solution for 1 hour and 10 μl drop of CON A solution was added only on the luminal side. After an hour of incubation at room temperature, CON A localization was analyzed by taking Z-stack images using confocal microscope (LSM 510 Meta; Carl Zeiss).

Ethics Statement. All experimental animal protocols were conducted in accordance with National Institutes of Health Guide for the care and use of laboratory animals and approved by the Institutional Animal Care and Use Committee at Johns Hopkins Medical School.

1. Parmar, K. M. *et al*. Integration of flow-dependent endothelial phenotypes by Kruppel-like factor 2. *J Clin Invest* **116**, 49–58 (2006).
2. Tzima, E. *et al*. A mechanosensory complex that mediates the endothelial cell response to fluid shear stress. *Nature* **437**, 426–431 (2005).
3. Seebach, J. *et al*. Endothelial barrier function under laminar fluid shear stress. *Lab Invest* **80**, 1819–1831 (2000).
4. Akimoto, S., Mitsumata, M., Sasaguri, T. & Yoshida, Y. Laminar shear stress inhibits vascular endothelial cell proliferation by inducing cyclin-dependent kinase inhibitor p21(Sdi1/Cip1/Waf1). *Circ Res* **86**, 185–190 (2000).
5. Dekker, R. J. *et al*. Prolonged fluid shear stress induces a distinct set of endothelial cell genes, most specifically lung Kruppel-like factor (KLF2). *Blood* **100**, 1689–1698 (2002).
6. Dekker, R. J. *et al*. KLF2 provokes a gene expression pattern that establishes functional quiescent differentiation of the endothelium. *Blood* **107**, 4354–4363 (2006).
7. Tsai, A. G., Johnson, P. C. & Intaglietta, M. Oxygen gradients in the microcirculation. *Physiol Rev* **83**, 933–963 (2003).
8. Matsumoto, S. *et al*. Simultaneous imaging of tumor oxygenation and microvascular permeability using Overhauser enhanced MRI. *Proc Natl Acad Sci U S A* **106**, 17898–17903 (2009).
9. Skuli, N. *et al*. Endothelial HIF-2alpha regulates murine pathological angiogenesis and revascularization processes. *J Clin Invest* **122**, 1427–1443 (2012).
10. Koto, T. *et al*. Hypoxia disrupts the barrier function of neural blood vessels through changes in the expression of claudin-5 in endothelial cells. *Am J Pathol* **170**, 1389–1397 (2007).
11. Abaci, H. E., Truitt, R., Luong, E., Drazer, G. & Gerecht, S. Adaptation to oxygen deprivation in cultures of human pluripotent stem cells, endothelial progenitor cells, and umbilical vein endothelial cells. *Am J Physiol Cell Physiol* **298**, C1527–1537 (2010).
12. Robinson, N. J. *et al*. Oxygen and the liberation of placental factors responsible for vascular compromise. *Lab Invest* **88**, 293–305 (2008).
13. Abaci, H. E., Drazer, G. & Gerecht, S. Recapitulating the vascular microenvironment in microfluidic platforms. *Nano LIFE* **03** (2013).
14. Huh, D. *et al*. A human disease model of drug toxicity-induced pulmonary edema in a lung-on-a-chip microdevice. *Sci Transl Med* **4**, 159ra147 (2012).
15. Zheng, Y. *et al*. In vitro microvessels for the study of angiogenesis and thrombosis. *Proc Natl Acad Sci U S A* **109**, 9342–9347 (2012).
16. Abaci, H. E., Devendra, R., Soman, R., Drazer, G. & Gerecht, S. Microbioreactors to manipulate oxygen tension and shear stress in the microenvironment of vascular stem and progenitor cells. *Biotechnol. Appl. Biochem.* **59**, 97–105 (2012).
17. Tian, C. *et al*. Resveratrol ameliorates high-glucose-induced hyperpermeability mediated by caveolae via VEGF/KDR pathway. *Genes Nutr* **8**, 231–239 (2013).
18. Daher, I. N. & Yeh, E. T. Vascular complications of selected cancer therapies. *Nat Clin Pract Cardiovasc Med* **5**, 797–805 (2008).
19. Ito, W. D. *et al*. Angiogenesis but not collateral growth is associated with ischemia after femoral artery occlusion. *Am J Physiol* **273**, H1255–1265 (1997).
20. Beck, H. & Plate, K. H. Angiogenesis after cerebral ischemia. *Acta Neuropathol* **117**, 481–496 (2009).
21. Mitsos, S. *et al*. Therapeutic angiogenesis for myocardial ischemia revisited: basic biological concepts and focus on latest clinical trials. *Angiogenesis* **15**, 1–22 (2012).
22. Fontanella, A. N. *et al*. Quantitative mapping of hemodynamics in the lung, brain, and dorsal window chamber-grown tumors using a novel, automated algorithm. *Microcirculation*, (2013).
23. Millan, J. *et al*. Adherens junctions connect stress fibres between adjacent endothelial cells. *BMC Biol* **8**, 11 (2010).
24. Noria, S., Cowan, D. B., Gotlieb, A. I. & Langille, B. L. Transient and steady-state effects of shear stress on endothelial cell adherens junctions. *Circ Res* **85**, 504–514 (1999).
25. Abaci, H. E., Devendra, R., Smith, Q., Gerecht, S. & Drazer, G. Design and development of microbioreactors for long-term cell culture in controlled oxygen microenvironments. *Biomed Microdevices* **14**, 145–152 (2012).
26. Prasain, N. & Stevens, T. The actin cytoskeleton in endothelial cell phenotypes. *Microvasc Res* **77**, 53–63 (2009).
27. Conway, D. E. *et al*. Fluid Shear Stress on Endothelial Cells Modulates Mechanical Tension across VE-Cadherin and PECAM-1. *Curr Biol* **23**, 1024–1030 (2013).
28. Fernandez-Martin, L. *et al*. Crosstalk between reticular adherens junctions and platelet endothelial cell adhesion molecule-1 regulates endothelial barrier function. *Arterioscler Thromb Vasc Biol* **32**, e90–102 (2012).

29. Lee, S. *et al.* Autocrine VEGF signaling is required for vascular homeostasis. *Cell* **130**, 691–703 (2007).
30. Longley, D. B., Harkin, D. P. & Johnston, P. G. 5-fluorouracil: mechanisms of action and clinical strategies. *Nat Rev Cancer* **3**, 330–338 (2003).
31. Hayward, R. *et al.* Training enhances vascular relaxation after chemotherapy-induced vasoconstriction. *Med Sci Sports Exerc* **36**, 428–434 (2004).
32. Han, R. *et al.* Systemic 5-fluorouracil treatment causes a syndrome of delayed myelin destruction in the central nervous system. *J Biol* **7**, 12 (2008).
33. Mosseri, M., Fingert, H. J., Varticovski, L., Chokshi, S. & Isner, J. M. In vitro evidence that myocardial ischemia resulting from 5-fluorouracil chemotherapy is due to protein kinase C-mediated vasoconstriction of vascular smooth muscle. *Cancer Res* **53**, 3028–3033 (1993).
34. Frampton, G. A., Lazcano, E. A., Li, H., Mohamad, A. & DeMorrow, S. Resveratrol enhances the sensitivity of cholangiocarcinoma to chemotherapeutic agents. *Lab Invest* **90**, 1325–1338 (2010).
35. Fulgenzi, A., Bertelli, A. A., Magni, E., Ferrero, E. & Ferrero, M. E. In vivo inhibition of TNFalpha-induced vascular permeability by resveratrol. *Transplant Proc* **33**, 2341–2343 (2001).
36. Rieder, S. A., Nagarkatti, P. & Nagarkatti, M. Multiple anti-inflammatory pathways triggered by resveratrol lead to amelioration of staphylococcal enterotoxin B-induced lung injury. *Br J Pharmacol* **167**, 1244–1258 (2012).
37. Hashimoto, T. & Pittet, J. F. Angiopoietin-2: modulator of vascular permeability in acute lung injury? *PLoS Med* **3**, e113 (2006).
38. Yuan, S. Y. *et al.* Myosin light chain phosphorylation in neutrophil-stimulated coronary microvascular leakage. *Circ Res* **90**, 1214–1221 (2002).
39. Low, B., Liang, M. & Fu, J. p38 mitogen-activated protein kinase mediates sidestream cigarette smoke-induced endothelial permeability. *J Pharmacol Sci* **104**, 225–231 (2007).
40. Zhang, X. L. *et al.* Resveratrol down-regulates Myosin light chain kinase, induces apoptosis and inhibits diethylnitrosamine-induced liver tumorigenesis in rats. *Int J Mol Sci* **14**, 1940–1951 (2013).
41. Lin, Z. *et al.* Kruppel-like factor 2 regulates endothelial barrier function. *Arterioscler Thromb Vasc Biol* **30**, 1952–1959 (2010).
42. Scholz, D. *et al.* Contribution of arteriogenesis and angiogenesis to postocclusive hindlimb perfusion in mice. *J Mol Cell Cardiol* **34**, 775–787 (2002).
43. Manalo, D. J. *et al.* Transcriptional regulation of vascular endothelial cell responses to hypoxia by HIF-1. *Blood* **105**, 659–669 (2005).
44. dela Paz, N. G., Walshe, T. E., Leach, L. L., Saint-Geniez, M. & D'Amore, P. A. Role of shear-stress-induced VEGF expression in endothelial cell survival. *J Cell Sci* **125**, 831–843 (2012).
45. Scharpfenecker, M., Fiedler, U., Reiss, Y. & Augustin, H. G. The Tie-2 ligand angiopoietin-2 destabilizes quiescent endothelium through an internal autocrine loop mechanism. *J Cell Sci* **118**, 771–780 (2005).
46. Estrada, R. *et al.* Endothelial cell culture model for replication of physiological profiles of pressure, flow, stretch, and shear stress in vitro. *Anal Chem* **83**, 3170–3177 (2011).
47. Khan, O. F. & Sefton, M. V. Endothelial cell behaviour within a microfluidic mimic of the flow channels of a modular tissue engineered construct. *Biomed Microdevices* **13**, 69–87 (2011).
48. Zhao, F., Sellgren, K. & Ma, T. Low-oxygen pretreatment enhances endothelial cell growth and retention under shear stress. *Tissue Eng Part C Methods* **15**, 135–146 (2009).
49. Jones, C. I., 3rd *et al.* Endothelial cell respiration is affected by the oxygen tension during shear exposure: role of mitochondrial peroxynitrite. *Am J Physiol Cell Physiol* **295**, C180–191 (2008).
50. Abaci, H. E., Truitt, R., Tan, S. & Gerecht, S. Unforeseen decreases in dissolved oxygen levels affect tube formation kinetics in collagen gels. *Am J Physiol Cell Physiol* **301**, C431–440 (2011).
51. Polk, A., Vaage-Nilsen, M., Vistisen, K. & Nielsen, D. L. Cardiotoxicity in cancer patients treated with 5-fluorouracil or capecitabine: A systematic review of incidence, manifestations and predisposing factors. *Cancer Treat Rev*, (2013).
52. Jensen, S. A. & Sorensen, J. B. 5-fluorouracil-based therapy induces endovascular injury having potential significance to development of clinically overt cardiotoxicity. *Cancer Chemother Pharmacol* **69**, 57–64 (2012).
53. Sudhoff, T. *et al.* 5-Fluorouracil induces arterial vasocontractions. *Ann Oncol* **15**, 661–664 (2004).
54. Sudoh, M. *et al.* A new animal model of continuous catheterization for investigating mechanisms of arteritis associated with chemotherapy. *Life Sci* **74**, 3025–3032 (2004).
55. Lamberti, M. *et al.* 5-Fluorouracil induces apoptosis in rat cardiocytes through intracellular oxidative stress. *J Exp Clin Cancer Res* **31**, 60 (2012).
56. Wada, H. *et al.* Combination of interferon-alpha and 5-fluorouracil inhibits endothelial cell growth directly and by regulation of angiogenic factors released by tumor cells. *BMC Cancer* **9**, 361 (2009).
57. Matthay, M. A., Ware, L. B. & Zimmerman, G. A. The acute respiratory distress syndrome. *J Clin Invest* **122**, 2731–2740 (2012).
58. van Bruggen, N. *et al.* VEGF antagonism reduces edema formation and tissue damage after ischemia/reperfusion injury in the mouse brain. *J Clin Invest* **104**, 1613–1620 (1999).
59. Chakroborty, D. *et al.* Dopamine stabilizes tumor blood vessels by up-regulating angiopoietin 1 expression in pericytes and Kruppel-like factor-2 expression in tumor endothelial cells. *Proc Natl Acad Sci U S A* **108**, 20730–20735 (2011).
60. Hayashi, T., Noshita, N., Sugawara, T. & Chan, P. H. Temporal profile of angiogenesis and expression of related genes in the brain after ischemia. *J Cereb Blood Flow Metab* **23**, 166–180 (2003).
61. Beck, H., Acker, T., Wiessner, C., Allegrini, P. R. & Plate, K. H. Expression of angiopoietin-1, angiopoietin-2, and tie receptors after middle cerebral artery occlusion in the rat. *Am J Pathol* **157**, 1473–1483 (2000).
62. Bhattacharya, R. *et al.* Inhibition of vascular permeability factor/vascular endothelial growth factor-mediated angiogenesis by the Kruppel-like factor KLF2. *J Biol Chem* **280**, 28848–28851 (2005).
63. Kawanami, D. *et al.* Kruppel-like factor 2 inhibits hypoxia-inducible factor 1alpha expression and function in the endothelium. *J Biol Chem* **284**, 20522–20530 (2009).
64. Fukumura, D. *et al.* Predominant role of endothelial nitric oxide synthase in vascular endothelial growth factor-induced angiogenesis and vascular permeability. *Proc Natl Acad Sci U S A* **98**, 2604–2609 (2001).
65. Kremer, C., Breier, G., Risau, W. & Plate, K. H. Up-regulation of flk-1/vascular endothelial growth factor receptor 2 by its ligand in a cerebral slice culture system. *Cancer Res* **57**, 3852–3859 (1997).
66. Bouloumie, A., Schini-Kerth, V. B. & Busse, R. Vascular endothelial growth factor up-regulates nitric oxide synthase expression in endothelial cells. *Cardiovasc Res* **41**, 773–780 (1999).
67. Noel, J. *et al.* PECAM-1 and caveolae form the mechanosensing complex necessary for NOX2 activation and angiogenic signaling with stopped flow in pulmonary endothelium. *Am J Physiol Lung Cell Mol Physiol* **305**, L805–818 (2013).
68. Pugh, C. W. & Ratcliffe, P. J. Regulation of angiogenesis by hypoxia: role of the HIF system. *Nat Med* **9**, 677–684 (2003).
69. Gracia-Sancho, J., Villarreal, G., Jr., Zhang, Y. & Garcia-Cardena, G. Activation of SIRT1 by resveratrol induces KLF2 expression conferring an endothelial vasoprotective phenotype. *Cardiovasc Res* **85**, 514–519 (2010).
70. Carpenter, A. E. *et al.* CellProfiler: image analysis software for identifying and quantifying cell phenotypes. *Genome Biol* **7**, R100 (2006).
71. Sale, S. *et al.* Pharmacokinetics in mice and growth-inhibitory properties of the putative cancer chemopreventive agent resveratrol and the synthetic analogue trans 3,4,5,4′-tetramethoxystilbene. *Br J Cancer* **90**, 736–744 (2004).
72. Jarugula, V. R., Lam, S. S. & Boudinot, F. D. Nonlinear pharmacokinetics of 5-fluorouracil in rats. *J Pharm Sci* **86**, 756–758 (1997).
73. van Nieuw Amerongen, G. P., Musters, R. J., Eringa, E. C., Sipkema, P. & van Hinsbergh, V. W. Thrombin-induced endothelial barrier disruption in intact microvessels: role of RhoA/Rho kinase-myosin phosphatase axis. *Am J Physiol Cell Physiol* **294**, C1234–1241 (2008).

Acknowledgments

Author contributions

H.E.A., Y.S. and S.G. designed the experiments. H.E.A., Y.S. and S.T. performed the experiments and analyzed the data. H.E.A. and S.G. wrote the paper.

Additional information